

The photophysics of alloxazine: A quantum chemical investigation in vacuum and solution

Electronic Supplementary Information

Susanne Salzmann and Christel M. Marian
*Institute of Theoretical and Computational Chemistry,
Heinrich Heine University Düsseldorf,
Universitätsstr. 1, D-40225 Düsseldorf, Germany**

(Dated: June 12, 2009)

*Electronic address: Christel.Marian@uni-duesseldorf.de; URL: <http://www.theochem.uni-duesseldorf.de>

I. EXPERIMENTAL DATA

(See Table I)

II. OPTIMIZED GEOMETRIES OF ALLOXAZINE WATER COMPLEXES

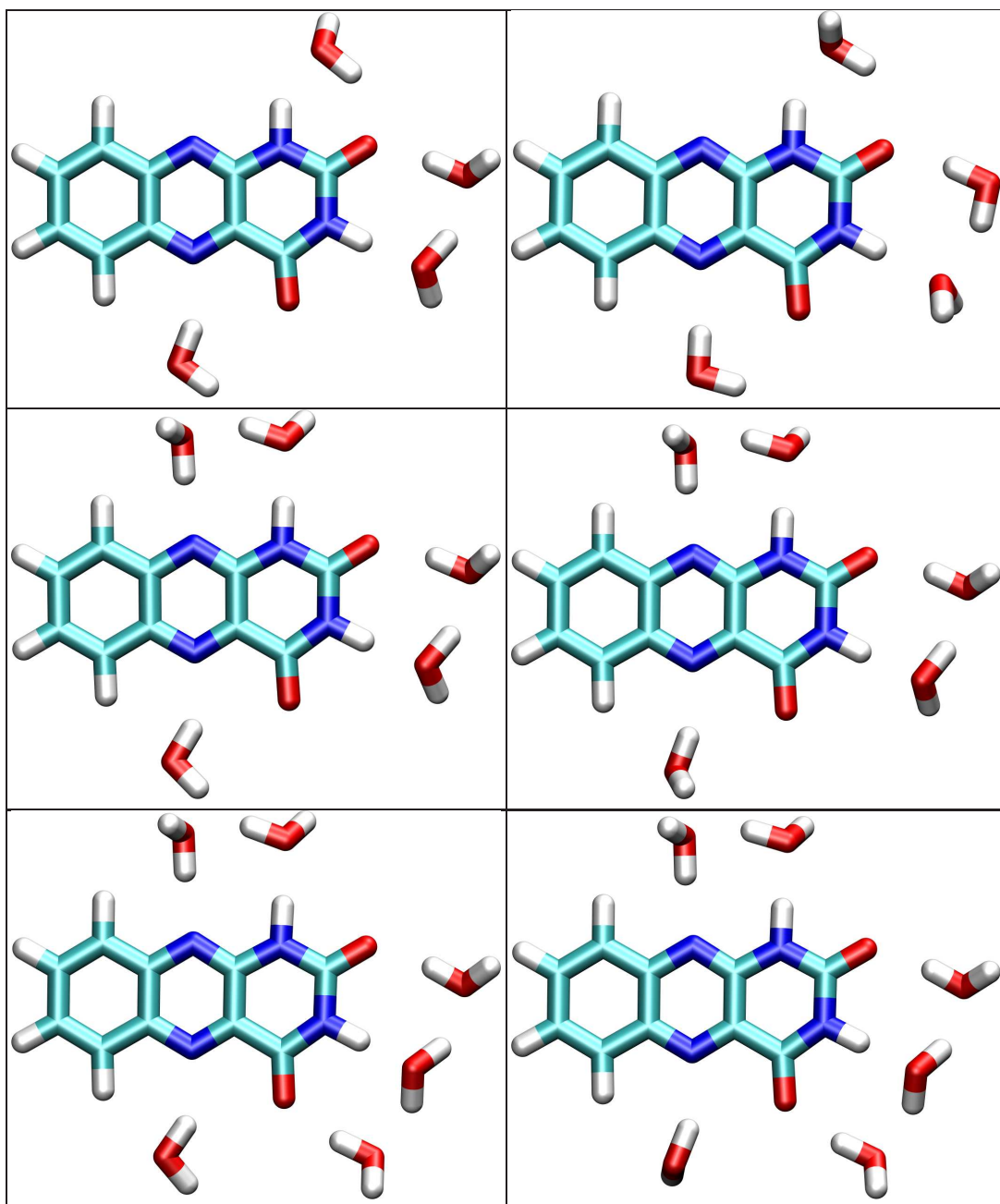


FIG. 1: AL: Optimized geometries of alloxazine water complexes. Left: micro-hydration, right: micro-hydration and COSMO.

TABLE I: Experimental spectroscopic data of alloxazine and lumichrome in various solvents. (Dx: 1,4-dioxane, DCE: 1,2-dichloroethane, AcN: acetonitrile, EtOH: ethanol, and MeOH: methanol.) In addition to the maxima of the first (λ_1) and second (λ_2) absorption bands and the fluorescence emission band (λ_F) [eV], fluorescence Φ_F and intersystem crossing Φ_{ISC} quantum yields, and fluorescence rate constants k_F [10^7 s $^{-1}$] are shown. (For comparison: lumiflavin in neutral aqueous solution $\Phi_{ISC}=0.67$ and $\Phi_F=0.29$ [1])

	AL						LC					
	Dx	DCE	AcN	EtOH	MeOH	H ₂ O	Dx	DCE	AcN	EtOH	MeOH	H ₂ O
ϵ	2.21	10.37	35.94	24.55	32.66	78.30	2.21	10.37	35.94	24.55	32.66	78.30
protic	-	-	-	+	+	+	-	-	-	+	+	+
λ_1	3.33 ^a	3.32 ^a	3.33 ^b	3.30 ^{c,d}	3.30 ^f	3.27 ^g	3.27 ^h	3.25 ^h	3.26 ^b	3.24 ^d	3.23 ^h	3.22 ^h
λ_2	3.89 ^a	3.85 ^a	3.87 ^b	3.84 ^c ,3.86 ^d	3.86 ^f	3.76 ^g	3.73 ^h	3.60 ^h	3.71 ^b	3.69 ^d	3.66 ^h	3.51 ^h
λ_F	2.85 ^a	2.86 ^a	2.87 ^b	2.79 ^d	-	-	2.79 ^h	2.81 ^h	2.84 ^b	2.74 ^d	2.74 ^h	2.59 ^h
Φ_F	-	0.023 ^a	0.009 ^b	0.033 ^{e,i} ,0.068 ^{e,j}	-	0.048 ^{k,m} ,0.033 ^{k,n}	0.027 ^h	0.026 ^h	0.028 ^b	0.067 ^{e,i} ,0.139 ^{e,j} ,0.036 ^k	0.032 ^h	0.088 ^h ,0.055 ^{k,m} ,0.034 ^{k,n}
Φ_{ISC}	-	-	0.36 ^l	-	-	0.45 ^{k,m} ,0.31 ^{k,n}	-	-	0.73 ^l	0.61 ^k	-	0.71 ^{k,m} ,0.44 ^{k,n}
k_F	-	12 ^a	2.6 ^b	-	1.8 ^a	3.3 ^{k,n}	6.0 ^h	4.3 ^h	4.3 ^h	4.2 ^k	3.0 ^h	3.2 ^h ,3.3 ^{k,n}

a : Ref. [2].

b : Ref. [3, 4].

c : Read from Ref. [5], Figure 9.

d : Ref. [6].

e : Ref. [5].

f : Ref. [7].

g : Read from Ref. [8], Figure 1.

h : Ref. [9].

i : 298 K.

j : 77 K.

k : Ref. [1].

l : Quantum yield of singlet oxygen formation, Ref. [3].

m : Estimates for pH 6.

n : At pH 2.

III. CALCULATION OF THE INTERSYSTEM CROSSING RATE CONSTANTS

In this appendix, we have assembled detailed information on the entities required for the evaluation of spin-forbidden nonradiative transition probabilities and on the sensitivity of the results with respect to technical parameters.

According to Toniolo and Persico [10, 11], it is possible to approximate the Fermi Golden Rule expression for the ISC rate constants k_{ISC} by a summation over rates of transition from the initial level $|i, \mathbf{v} = \mathbf{0}\rangle$ to individual final vibronic levels $|f, \mathbf{v}'\rangle$ in an energy interval of width 2η around the energy $E_{i, \mathbf{v}=\mathbf{0}}$. Here, the vectors \mathbf{v} and \mathbf{v}' represent sets of vibrational quantum numbers in all normal modes of the initial (i) and final (f) electronic state, respectively. If we denote the coupling matrix elements driving the radiationless transition by $H_{\mathbf{v}=\mathbf{0}, \mathbf{v}' }^{SO}$, the rate constant is obtained as

$$k_{ISC}(i \rightsquigarrow f) = \frac{2\pi}{\hbar\eta} \sum_{|E_{f, \mathbf{v}'} - E_{i, \mathbf{v}=\mathbf{0}}| < \eta} |H_{\mathbf{v}=\mathbf{0}, \mathbf{v}'}^{SO}|^2. \quad (1)$$

$H_{\mathbf{v}=\mathbf{0}, \mathbf{v}'}^{SO}$ can be expanded in a Taylor series in the variables $\{q_\kappa\}$, the normal coordinates, around some reference point \mathbf{q}_0 [12] which we have chosen to coincide with the minimum of the S_1 state.

$$\begin{aligned} H_{\mathbf{v}=\mathbf{0}, \mathbf{v}'}^{SO} &= \left\langle i \left| \hat{\mathcal{H}}_{SO} \right| f \right\rangle_{\mathbf{q}_0=\mathbf{0}} \langle \mathbf{v} = \mathbf{0} | \mathbf{v}' \rangle \\ &+ \sum_{\kappa} \left(\frac{\partial}{\partial q_\kappa} \langle i | \hat{\mathcal{H}}_{SO} | f \rangle \right)_{\mathbf{q}_0=\mathbf{0}} \langle \mathbf{v} = \mathbf{0} | q_\kappa | \mathbf{v}' \rangle \\ &+ O(|\mathbf{q}|^2) \end{aligned} \quad (2)$$

The first term on the right-hand side of equation (2) is a purely electronic matrix element and is denominated direct spin-orbit coupling in the following, whereas the term in the second line of equation (2) represents the first-order derivative coupling and is named vibronic spin-orbit coupling.

Tables II and III lists harmonic frequencies of the 19 out-of-plane vibrations in the first excited $^1(\pi \rightarrow \pi^*)$ and $^1(n \rightarrow \pi^*)$ states (coupling modes for the vibronic spin-orbit interaction) and the derivatives of the spin-orbit coupling matrix elements with respect to distortions along their normal coordinates.

The first-order derivatives of the SOMEs were calculated numerically by finite difference techniques, more precisely, by means of the symmetrized two-point formula:

$$\frac{\partial}{\partial q_\kappa} \left\langle i \left| \hat{\mathcal{H}}_{SO} \right| f \right\rangle_{\mathbf{q}_0} \approx \frac{\left\langle i \left| \hat{\mathcal{H}}_{SO} \right| f \right\rangle_{\mathbf{q}_0 + \epsilon \mathbf{e}_\kappa} - \left\langle i \left| \hat{\mathcal{H}}_{SO} \right| f \right\rangle_{\mathbf{q}_0 - \epsilon \mathbf{e}_\kappa}}{2\epsilon} \quad (3)$$

Here, \mathbf{e}_κ denotes the unit vector pointing into the direction of the normal mode v_κ . (For more details see Ref. [13].) Thus, single-point DFT/MRCI and subsequent Spock runs have to be carried out at two distorted molecular geometries $\mathbf{q}_0 \pm \epsilon \mathbf{e}_\kappa$ for each normal mode. For obtaining the derivatives employed in the final computations of the ISC rate constants, the displacement increment ϵ is set to a numerical value of 0.1 (referring to dimensionless normal mode coordinates \mathbf{q}_κ). In order to minimize the errors induced by numerical noise, the CI

space from a preceding DFT/MRCI run without symmetry constraints at the reference geometry \mathbf{q}_0 is used in all calculations. The molecular orbitals employed in the single-point CI calculations are reoptimized for the distorted geometries, of course.

Since the oop distortion exhibits a symmetric potential well, we do not expect a deviation between the SOME at two distorted molecular geometries $\mathbf{q}_0 \pm \epsilon \mathbf{e}_\kappa$. For our calculations in the vacuum this is fulfilled. There, in most cases, we find the difference between the two SOME to be less than 0.00001 cm⁻¹. For our calculations of the SOME derivatives in aqueous solution with COSMO, however, larger deviations between the two SOMEs turn up. This has been reported before and can be explained by the fact that the cavity construction for the COSMO calculation uses coordinates that are slightly distorted.[14] Although it would be desirable to obtain the derivatives of the SOME with COSMO with a higher precision, the induced errors do not change the order of magnitude of the resulting ISC rate constant, only its prefactor, as shown in Ref. [14] (Supplementary Information, Table 5).

Information about the parameters chosen in the calculation of the rate constants for the nonradiative transitions from $^1(n\pi^*)$ and $^1(\pi_H\pi_L^*)$ to the individual spin components of the $^3(\pi_H\pi_L^*)$, $^3(n\pi^*)$ and $^3(\pi_{H-1}\pi_L^*)$ states and the dependence of the results on these parameters are contained in Table IV to Table VII. A zero number of derivative coupling modes indicates direct spin-orbit coupling, nonzero numbers vibronic spin-orbit coupling.

TABLE II: AL: Harmonic frequencies ν_i [cm^{-1}] of the out-of-plane vibrational modes for the $^1(n\pi^*)$ and $^1(\pi_H\pi_L^*)$ states in the gas phase. Derivatives of SOMEs [$-i\text{cm}^{-1}$] with respect to the (dimensionless) normal coordinates at the corresponding equilibrium geometry q_0 .

$^1(n\pi^*)$				$^1(\pi_H\pi_L^*)$					
$\frac{\partial \langle ^1(n\pi^*) \hat{H}_{SO} ^3(n\pi^*) \rangle}{\partial q_i}$				$\frac{\partial \langle ^1(\pi_H\pi_L^*) \hat{H}_{SO} ^3(\pi_H\pi_L^*) \rangle}{\partial q_i}$					
mode	$\hat{\nu}_i$	(x)	(y)	mode	$\hat{\nu}_i$	(x)	(y)	(x)	(y)
1	72.15	-0.35	0.18	1	50 ^a	3.54	-1.22	-24.38	21.84
2	75.27	2.54	-0.31	2	67.92	-0.42	0.34	-31.48	33.06
3	137.73	-2.20	1.47	3	77.74	-0.10	-0.01	-26.78	28.06
4	151.84	-0.62	0.39	4	127.31	-0.54	-0.04	25.49	-25.87
6	180.98	4.69	-1.61	5	144.41	0.29	-0.07	27.41	-28.93
7	207.66	4.82	-1.95	7	223.02	-0.42	0.21	24.34	-24.94
8	330.88	-2.19	0.62	8	268.73	1.63	-1.00	-25.59	25.65
11	415.08	4.55	-1.05	10	337.94	0.81	-0.49	-24.23	24.63
13	477.36	0.19	0.20	12	405.52	1.33	-0.78	-25.01	25.29
14	498.66	-0.72	0.50	14	488.15	-0.51	0.27	24.12	-24.88
18	543.65	0.72	0.12	19	593.50	-0.38	0.16	24.47	-25.40
19	578.99	3.90	-1.15	20	642.08	1.09	-0.75	23.63	-25.40
21	612.81	0.07	0.27	21	651.09	0.41	-0.05	-24.53	25.37
23	661.55	-0.92	0.57	23	672.55	0.41	-0.23	-24.68	25.56
25	733.38	-0.38	-0.21	25	709.68	0.95	-0.66	-24.31	25.15
27	743.02	0.14	0.57	26	740.68	-0.15	-0.00 ^b	25.22	-26.21
28	768.35	5.06	-1.60	28	779.01	0.67	-0.45	24.64	-25.89
30	886.27	1.29	-0.56	30	900.97	-0.13	0.18	21.12	-22.17
32	930.61	-0.91	0.29	32	916.89	-0.24	0.09	23.60	-24.37

a: The TDDFT (B3LYP) PEH exhibits a very flat double well shape along mode 1 with a slightly imaginary frequency (see text). The setting $\hat{\nu}_i$ represents an approximate harmonic model of the $^1(\pi_H\pi_L^*)$ state PEH along mode 1. Such an imaginary frequency in the initial state, where only $v = 0$ plays a role, does not change the vibrational density of states.

b: Absolute value of the derivative lower than 0.01 cm^{-1}

TABLE III: AL: Harmonic frequencies ν_i [cm^{-1}] of the out-of-plane vibrational modes for the $^1(n\pi^*)$ and $^1(\pi_H\pi_L^*)$ states in aqueous solution. Derivatives of SOMEs [$-i\text{cm}^{-1}$] with respect to the (dimensionless) normal coordinates at the corresponding equilibrium geometry q_0 .

$^1(n\pi^*)$				$^1(\pi_H\pi_L^*)$					
$\frac{\partial \langle ^1(n\pi^*) \hat{H}_{SO} ^3(n\pi^*) \rangle}{\partial q_i}$				$\frac{\partial \langle ^1(\pi_H\pi_L^*) \hat{H}_{SO} ^3(\pi_H\pi_L^*) \rangle}{\partial q_i}$					
mode	$\hat{\nu}_i$	(x)	(y)	mode	$\hat{\nu}_i$	(x)	(y)	(x)	(y)
1	72.15	0.73	-0.00 ^b	1	50 ^a	1.24	-0.41	1.13	-0.20
2	75.27	1.70	-1.26	2	67.92	-0.20	0.21	-0.10	0.03
3	137.73	-5.96	2.22	3	77.74	-0.11	0.00	0.03	-0.02
4	151.84	-0.60	0.56	4	127.31	-0.27	-0.10	-0.47	-0.15
6	180.98	5.91	-2.98	5	144.41	0.15	-0.09	-0.05	0.11
7	207.66	11.84	-4.10	7	223.02	-0.21	0.12	-0.62	0.24
8	330.88	-2.59	1.33	8	268.73	0.89	-0.62	1.31	-0.62
11	415.08	0.92	-2.19	10	337.94	0.51	-0.34	0.92	-0.50
13	477.36	1.98	-0.74	12	405.52	0.60	-0.43	1.15	-0.71
14	498.66	-0.72	0.12	14	488.15	-0.29	0.17	-0.74	0.49
18	543.65	1.86	-0.59	19	593.50	-0.15	0.01	-0.40	0.26
19	578.99	3.13	-2.05	20	642.08	0.57	-0.43	0.14	0.24
21	612.81	-1.17	0.43	21	651.09	0.23	0.01	0.69	-0.52
23	661.55	-0.04	0.72	23	672.55	0.25	-0.17	0.45	-0.31
25	733.38	-0.56	0.06	25	709.68	0.54	-0.47	0.43	-0.40
27	743.02	-1.42	0.30	26	740.68	-0.07	0.00	-0.17	0.14
28	768.35	8.87	-4.27	28	779.01	0.52	-0.38	-0.50	0.29
30	886.27	3.00	-1.31	30	900.97	-0.12	0.09	-0.07	0.12
32	930.61	-1.93	0.82	32	916.89	-0.02	-0.03	-0.41	0.16

a: The TDDFT (B3LYP) PEH exhibits a very flat double well shape along mode 1 with a slightly imaginary frequency (see text). The setting $\hat{\nu}_i$ represents an approximate harmonic model of the $^1(\pi_H\pi_L^*)$ state PEH along mode 1. Such an imaginary frequency in the initial state, where only $v = 0$ plays a role, does not change the vibrational density of states.

b: Absolute value of the derivative lower than 0.01 cm^{-1}

TABLE IV: AL: Calculated rate constants k_{ISC} [s^{-1}] for (S \rightsquigarrow T) ISC channels of the $^1(n\pi^*)$ state in the vacuum. Remaining columns: adiabatic electronic energy difference ΔE^{ad} [eV], direct SOME $| \langle i | \hat{H}_{SO} | f \rangle |_{q_0}$ [cm^{-1}], number $\#derivs$ of included derivatives w.r.t. *oop* modes in vibronic SO coupling, number $\#acc$ of included accepting modes, width η [cm^{-1}] of search interval, resulting number $\#v'$ of final state vibrational levels within search interval.

channel $i \rightsquigarrow f$	parameters & and settings					results	
	- ΔE^{ad}	direct SO $ \langle i \hat{H}_{SO} f \rangle _{q_0}$	vib. SO acceptors $\#derivs$	interval $\#acc$	η	levels $\#v'$	rate k_{ISC}
$^1(n\pi^*) \rightsquigarrow ^3(\pi_H \pi_L^*)_x$	6222	11.67	-	41	0.0001	20	$4.7 \cdot 10^9$
$^1(n\pi^*) \rightsquigarrow ^3(\pi_H \pi_L^*)_x$	6222	11.67	-	41	0.001	183	$2.1 \cdot 10^9$
$^1(n\pi^*) \rightsquigarrow ^3(\pi_H \pi_L^*)_x$	6222	11.67	-	41	0.01	1902	$1.6 \cdot 10^9$
$^1(n\pi^*) \rightsquigarrow ^3(\pi_H \pi_L^*)_x$	6222	11.67	-	41	0.1	19481	$1.2 \cdot 10^{10}$
$^1(n\pi^*) \rightsquigarrow ^3(\pi_H \pi_L^*)_x$	6222	11.67	-	41	1	194900	$1.3 \cdot 10^{10}$
$^1(n\pi^*) \rightsquigarrow ^3(\pi_H \pi_L^*)_y$	6222	-4.28	-	41	0.0001	20	$6.4 \cdot 10^8$
$^1(n\pi^*) \rightsquigarrow ^3(\pi_H \pi_L^*)_y$	6222	-4.28	-	41	0.001	183	$2.9 \cdot 10^8$
$^1(n\pi^*) \rightsquigarrow ^3(\pi_H \pi_L^*)_y$	6222	-4.28	-	41	0.01	1902	$2.1 \cdot 10^8$
$^1(n\pi^*) \rightsquigarrow ^3(\pi_H \pi_L^*)_y$	6222	-4.28	-	41	0.1	19481	$1.7 \cdot 10^9$
$^1(n\pi^*) \rightsquigarrow ^3(\pi_H \pi_L^*)_y$	6222	-4.28	-	41	1	194900	$1.8 \cdot 10^9$
$^1(n\pi^*) \rightsquigarrow ^3(\pi_H \pi_L^*)_z$	6222	-	-	-	-	-	-
$^1(n\pi^*) \rightsquigarrow ^3(n\pi^*)_x$	3422	-	19	41	0.001	200	$3.1 \cdot 10^4$
$^1(n\pi^*) \rightsquigarrow ^3(n\pi^*)_x$	3422	-	19	41	0.01	2103	$2.6 \cdot 10^8$
$^1(n\pi^*) \rightsquigarrow ^3(n\pi^*)_x$	3422	-	19	41	0.1	20984	$3.9 \cdot 10^8$
$^1(n\pi^*) \rightsquigarrow ^3(n\pi^*)_x$	3422	-	19	41	1	211340	$4.0 \cdot 10^7$
$^1(n\pi^*) \rightsquigarrow ^3(n\pi^*)_y$	3422	-	19	41	0.001	200	$2.8 \cdot 10^4$
$^1(n\pi^*) \rightsquigarrow ^3(n\pi^*)_y$	3422	-	19	41	0.01	2103	$2.8 \cdot 10^7$
$^1(n\pi^*) \rightsquigarrow ^3(n\pi^*)_y$	3422	-	19	41	0.1	20984	$8.8 \cdot 10^6$
$^1(n\pi^*) \rightsquigarrow ^3(n\pi^*)_y$	3422	-	19	41	1	211340	$5.7 \cdot 10^6$
$^1(n\pi^*) \rightsquigarrow ^3(n\pi^*)_z$	3422	-0.19	-	41	0.01	5	$2.1 \cdot 10^4$
$^1(n\pi^*) \rightsquigarrow ^3(n\pi^*)_z$	3422	-0.19	-	41	0.1	53	$8.9 \cdot 10^4$
$^1(n\pi^*) \rightsquigarrow ^3(n\pi^*)_z$	3422	-0.19	-	41	1	562	$9.5 \cdot 10^4$
$^1(n\pi^*) \rightsquigarrow ^3(\pi_{H-1} \pi_L^*)_x$	2634	1.48	-	41	1	4	$3.2 \cdot 10^8$
$^1(n\pi^*) \rightsquigarrow ^3(\pi_{H-1} \pi_L^*)_x$	2634	1.48	-	41	10	37	$2.1 \cdot 10^8$
$^1(n\pi^*) \rightsquigarrow ^3(\pi_{H-1} \pi_L^*)_x$	2634	1.48	-	41	100	420	$2.7 \cdot 10^8$
$^1(n\pi^*) \rightsquigarrow ^3(\pi_{H-1} \pi_L^*)_y$	2634	9.56	-	41	1	4	$1.3 \cdot 10^{10}$
$^1(n\pi^*) \rightsquigarrow ^3(\pi_{H-1} \pi_L^*)_y$	2634	9.56	-	41	10	37	$8.8 \cdot 10^9$
$^1(n\pi^*) \rightsquigarrow ^3(\pi_{H-1} \pi_L^*)_y$	2634	9.56	-	41	100	420	$1.1 \cdot 10^{10}$
$^1(n\pi^*) \rightsquigarrow ^3(\pi_{H-1} \pi_L^*)_z$	2634	-	-	-	-	-	-

TABLE V: AL: Calculated rate constants k_{ISC} [s^{-1}] for (S \rightsquigarrow T) ISC channels of the $^1(\pi_H\pi_L^*)$ state in the vacuum. Remaining columns: adiabatic electronic energy difference ΔE^{ad} [eV], direct SOME $\langle i|\hat{H}_{SO}|f\rangle|_{q_0}$ [cm^{-1}], number $\#derivs$ of included derivatives w.r.t. *oop* modes in vibronic SO coupling, number $\#acc$ of included accepting modes, width η [cm^{-1}] of search interval, resulting number $\#v'$ of final state vibrational levels within search interval.

channel $i \rightsquigarrow f$	parameters & and settings					results	
	ΔE^{ad}	direct SO $\langle i \hat{H}_{SO} f\rangle _{q_0}$	vib. SO	acceptors	interval η	levels $\#v'$	rate k_{ISC}
$^1(\pi_H\pi_L^*) \rightsquigarrow ^3(\pi_H\pi_L^*)_x$	6776	-	19	41	0.0001	1769	$3.8 \cdot 10^5$
$^1(\pi_H\pi_L^*) \rightsquigarrow ^3(\pi_H\pi_L^*)_x$	6776	-	19	41	0.001	17994	$1.1 \cdot 10^6$
$^1(\pi_H\pi_L^*) \rightsquigarrow ^3(\pi_H\pi_L^*)_x$	6776	-	19	41	0.01	178603	$2.8 \cdot 10^6$
$^1(\pi_H\pi_L^*) \rightsquigarrow ^3(\pi_H\pi_L^*)_y$	6776	-	19	41	0.0001	1769	$8.4 \cdot 10^4$
$^1(\pi_H\pi_L^*) \rightsquigarrow ^3(\pi_H\pi_L^*)_y$	6776	-	19	41	0.001	17994	$2.6 \cdot 10^5$
$^1(\pi_H\pi_L^*) \rightsquigarrow ^3(\pi_H\pi_L^*)_y$	6776	-	19	41	0.01	178603	$5.5 \cdot 10^5$
$^1(\pi_H\pi_L^*) \rightsquigarrow ^3(\pi_H\pi_L^*)_z$	6776	-0.01	-	41	0.01	5305	9.8
$^1(\pi_H\pi_L^*) \rightsquigarrow ^3(\pi_H\pi_L^*)_z$	6776	-0.01	-	41	0.1	53152	$1.8 \cdot 10^1$
$^1(\pi_H\pi_L^*) \rightsquigarrow ^3(\pi_H\pi_L^*)_z$	6776	-0.01	-	41	1	531576	$4.3 \cdot 10^1$
$^1(\pi_H\pi_L^*) \rightsquigarrow ^3(n\pi^*)_x$	3646	-3.43	-	41	0.001	1	$2.7 \cdot 10^6$
$^1(\pi_H\pi_L^*) \rightsquigarrow ^3(n\pi^*)_x$	3646	-3.43	-	41	0.01	9	$7.5 \cdot 10^7$
$^1(\pi_H\pi_L^*) \rightsquigarrow ^3(n\pi^*)_x$	3646	-3.43	-	41	0.1	83	$2.4 \cdot 10^9$
$^1(\pi_H\pi_L^*) \rightsquigarrow ^3(n\pi^*)_x$	3646	-3.43	-	41	1	992	$8.7 \cdot 10^8$
$^1(\pi_H\pi_L^*) \rightsquigarrow ^3(n\pi^*)_y$	3646	3.59	-	41	0.001	1	$3.0 \cdot 10^6$
$^1(\pi_H\pi_L^*) \rightsquigarrow ^3(n\pi^*)_y$	3646	3.59	-	41	0.01	9	$8.2 \cdot 10^7$
$^1(\pi_H\pi_L^*) \rightsquigarrow ^3(n\pi^*)_y$	3646	3.59	-	41	0.1	83	$2.6 \cdot 10^9$
$^1(\pi_H\pi_L^*) \rightsquigarrow ^3(n\pi^*)_y$	3646	3.59	-	41	1	992	$9.6 \cdot 10^8$
$^1(\pi_H\pi_L^*) \rightsquigarrow ^3(n\pi^*)_z$	3646	-	-	-	-	-	-
$^1(\pi_H\pi_L^*) \rightsquigarrow ^3(\pi_{H-1}\pi_L^*)_x$	3188	-	19	41	0.01	12	$1.4 \cdot 10^9$
$^1(\pi_H\pi_L^*) \rightsquigarrow ^3(\pi_{H-1}\pi_L^*)_x$	3188	-	19	41	0.1	96	$4.0 \cdot 10^9$
$^1(\pi_H\pi_L^*) \rightsquigarrow ^3(\pi_{H-1}\pi_L^*)_x$	3188	-	19	41	1	1045	$9.0 \cdot 10^{10}$
$^1(\pi_H\pi_L^*) \rightsquigarrow ^3(\pi_{H-1}\pi_L^*)_x$	3188	-	19	41	10	10395	$3.2 \cdot 10^{11}$
$^1(\pi_H\pi_L^*) \rightsquigarrow ^3(\pi_{H-1}\pi_L^*)_x$	3188	-	19	41	100	106107	$2.6 \cdot 10^{11}$
$^1(\pi_H\pi_L^*) \rightsquigarrow ^3(\pi_{H-1}\pi_L^*)_y$	3188	-	19	41	0.01	12	$1.6 \cdot 10^9$
$^1(\pi_H\pi_L^*) \rightsquigarrow ^3(\pi_{H-1}\pi_L^*)_y$	3188	-	19	41	0.1	96	$5.2 \cdot 10^9$
$^1(\pi_H\pi_L^*) \rightsquigarrow ^3(\pi_{H-1}\pi_L^*)_y$	3188	-	19	41	1	1045	$9.7 \cdot 10^{10}$
$^1(\pi_H\pi_L^*) \rightsquigarrow ^3(\pi_{H-1}\pi_L^*)_y$	3188	-	19	41	10	10395	$3.5 \cdot 10^{11}$
$^1(\pi_H\pi_L^*) \rightsquigarrow ^3(\pi_{H-1}\pi_L^*)_y$	3188	-	19	41	100	106107	$2.8 \cdot 10^{11}$
$^1(\pi_H\pi_L^*) \rightsquigarrow ^3(\pi_{H-1}\pi_L^*)_z$	3188	<0.01	-	41	1	22	$2.0 \cdot 10^{-1}$
$^1(\pi_H\pi_L^*) \rightsquigarrow ^3(\pi_{H-1}\pi_L^*)_z$	3188	<0.01	-	41	10	206	$3.3 \cdot 10^{-1}$
$^1(\pi_H\pi_L^*) \rightsquigarrow ^3(\pi_{H-1}\pi_L^*)_z$	3188	<0.01	-	41	100	2107	$4.0 \cdot 10^{-1}$

TABLE VI: AL: Calculated rate constants k_{ISC} [s^{-1}] for ($S \rightsquigarrow Tn$) ISC channels of the $^1(n\pi^*)$ state in aqueous solution. Remaining columns: adiabatic electronic energy difference ΔE^{ad} [eV], direct SOME $| \langle i | \hat{H}_{SO} | f \rangle |_{q_0}$ [cm^{-1}], number $\#derivs$ of included derivatives w.r.t. *oop* modes in vibronic SO coupling, number $\#acc$ of included accepting modes, width η [cm^{-1}] of search interval, resulting number $\#v'$ of final state vibrational levels within search interval.

channel $i \rightsquigarrow f$	parameters & and settings					results	
	- ΔE^{ad}	direct SO $ \langle i \hat{H}_{SO} f \rangle _{q_0}$	vib. SO	acceptors $\#acc$	interval η	levels $\#v'$	rate k_{ISC}
$^1(n\pi^*) \rightsquigarrow ^3(\pi_H\pi_L^*)_x$	9047	11.06	-	41	0.0001	2104	$7.7 \cdot 10^8$
$^1(n\pi^*) \rightsquigarrow ^3(\pi_H\pi_L^*)_x$	9047	11.06	-	41	0.001	21800	$7.1 \cdot 10^9$
$^1(n\pi^*) \rightsquigarrow ^3(\pi_H\pi_L^*)_x$	9047	11.06	-	41	0.01	220317	$9.6 \cdot 10^9$
$^1(n\pi^*) \rightsquigarrow ^3(\pi_H\pi_L^*)_x$	9047	11.06	-	41	0.1	2202844	$1.0 \cdot 10^{10}$
$^1(n\pi^*) \rightsquigarrow ^3(\pi_H\pi_L^*)_y$	9047	-4.76	-	41	0.0001	2104	$1.0 \cdot 10^7$
$^1(n\pi^*) \rightsquigarrow ^3(\pi_H\pi_L^*)_y$	9047	-4.76	-	41	0.001	21800	$9.5 \cdot 10^7$
$^1(n\pi^*) \rightsquigarrow ^3(\pi_H\pi_L^*)_y$	9047	-4.76	-	41	0.01	220317	$1.3 \cdot 10^8$
$^1(n\pi^*) \rightsquigarrow ^3(\pi_H\pi_L^*)_y$	9047	-4.76	-	41	0.1	2202844	$1.4 \cdot 10^8$
$^1(n\pi^*) \rightsquigarrow ^3(\pi_H\pi_L^*)_z$	9047	-	-	-	-	-	-
$^1(n\pi^*) \rightsquigarrow ^3(n\pi^*)_x$	2525	-	19	41	0.001	14	$1.8 \cdot 10^7$
$^1(n\pi^*) \rightsquigarrow ^3(n\pi^*)_x$	2525	-	19	41	0.01	126	$2.3 \cdot 10^9$
$^1(n\pi^*) \rightsquigarrow ^3(n\pi^*)_x$	2525	-	19	41	0.1	1381	$3.5 \cdot 10^8$
$^1(n\pi^*) \rightsquigarrow ^3(n\pi^*)_x$	2525	-	19	41	1	13747	$3.8 \cdot 10^8$
$^1(n\pi^*) \rightsquigarrow ^3(n\pi^*)_y$	2525	-	19	41	0.001	14	$1.1 \cdot 10^5$
$^1(n\pi^*) \rightsquigarrow ^3(n\pi^*)_y$	2525	-	19	41	0.01	126	$4.2 \cdot 10^8$
$^1(n\pi^*) \rightsquigarrow ^3(n\pi^*)_y$	2525	-	19	41	0.1	1381	$5.4 \cdot 10^7$
$^1(n\pi^*) \rightsquigarrow ^3(n\pi^*)_y$	2525	-	19	41	1	13747	$8.3 \cdot 10^7$
$^1(n\pi^*) \rightsquigarrow ^3(n\pi^*)_z$	2525	-0.16	-	41	0.1	8	$3.7 \cdot 10^1$
$^1(n\pi^*) \rightsquigarrow ^3(n\pi^*)_z$	2525	-0.16	-	41	1	65	$6.6 \cdot 10^4$
$^1(n\pi^*) \rightsquigarrow ^3(n\pi^*)_z$	2525	-0.16	-	41	10	595	$6.5 \cdot 10^4$
$^1(n\pi^*) \rightsquigarrow ^3(\pi_{H-1}\pi_L^*)_x$	5194	-3.71	-	41	0.1	264	$3.0 \cdot 10^9$
$^1(n\pi^*) \rightsquigarrow ^3(\pi_{H-1}\pi_L^*)_x$	5194	-3.71	-	41	1	2624	$1.3 \cdot 10^9$
$^1(n\pi^*) \rightsquigarrow ^3(\pi_{H-1}\pi_L^*)_x$	5194	-3.71	-	41	10	25807	$1.7 \cdot 10^9$
$^1(n\pi^*) \rightsquigarrow ^3(\pi_{H-1}\pi_L^*)_y$	5194	-2.38	-	41	0.1	264	$1.3 \cdot 10^9$
$^1(n\pi^*) \rightsquigarrow ^3(\pi_{H-1}\pi_L^*)_y$	5194	-2.38	-	41	1	2624	$7.0 \cdot 10^8$
$^1(n\pi^*) \rightsquigarrow ^3(\pi_{H-1}\pi_L^*)_y$	5194	-2.38	-	41	10	25807	$5.4 \cdot 10^8$
$^1(n\pi^*) \rightsquigarrow ^3(\pi_{H-1}\pi_L^*)_z$	5194	-	-	-	-	-	-

TABLE VII: AL: Calculated rate constants k_{ISC} [s^{-1}] for ($S \rightsquigarrow Tn$) ISC channels of the $^1(\pi_H\pi_L^*)$ state in aqueous solution. Remaining columns: adiabatic electronic energy difference ΔE^{ad} [eV], direct SOME $|\langle i|\hat{H}_{SO}|f\rangle|_{q_0}$ [cm^{-1}], number $\#derivs$ of included derivatives w.r.t. *oop* modes in vibronic SO coupling, number $\#acc$ of included accepting modes, width η [cm^{-1}] of search interval, resulting number $\#v'$ of final state vibrational levels within search interval.

channel $i \rightsquigarrow f$	parameters & and settings					results	
	- ΔE^{ad}	direct SO $ \langle i \hat{H}_{SO} f\rangle _{q_0}$	vib. SO acceptors $\#derivs$	interval $\#acc$	η	levels $\#v'$	rate k_{ISC}
$^1(\pi_H\pi_L^*) \rightsquigarrow ^3(\pi_H\pi_L^*)_x$	6615	-	19	41	0.0001	1355	$1.3 \cdot 10^5$
$^1(\pi_H\pi_L^*) \rightsquigarrow ^3(\pi_H\pi_L^*)_x$	6615	-	19	41	0.001	13316	$2.4 \cdot 10^5$
$^1(\pi_H\pi_L^*) \rightsquigarrow ^3(\pi_H\pi_L^*)_x$	6615	-	19	41	0.01	133013	$5.7 \cdot 10^5$
$^1(\pi_H\pi_L^*) \rightsquigarrow ^3(\pi_H\pi_L^*)_y$	6615	-	19	41	0.0001	1355	$8.0 \cdot 10^4$
$^1(\pi_H\pi_L^*) \rightsquigarrow ^3(\pi_H\pi_L^*)_y$	6615	-	19	41	0.001	13316	$9.4 \cdot 10^4$
$^1(\pi_H\pi_L^*) \rightsquigarrow ^3(\pi_H\pi_L^*)_y$	6615	-	19	41	0.01	133013	$1.4 \cdot 10^5$
$^1(\pi_H\pi_L^*) \rightsquigarrow ^3(\pi_H\pi_L^*)_z$	6615	-0.01	-	41	0.01	4019	7.8
$^1(\pi_H\pi_L^*) \rightsquigarrow ^3(\pi_H\pi_L^*)_z$	6615	-0.01	-	41	0.1	40084	$5.7 \cdot 10^1$
$^1(\pi_H\pi_L^*) \rightsquigarrow ^3(\pi_H\pi_L^*)_z$	6615	-0.01	-	41	1	399325	$6.9 \cdot 10^1$
$^1(\pi_H\pi_L^*) \rightsquigarrow ^3(\pi_{H-1}\pi_L^*)_x$	2762	-	19	41	0.1	17	$6.3 \cdot 10^5$
$^1(\pi_H\pi_L^*) \rightsquigarrow ^3(\pi_{H-1}\pi_L^*)_x$	2762	-	19	41	1	257	$9.5 \cdot 10^7$
$^1(\pi_H\pi_L^*) \rightsquigarrow ^3(\pi_{H-1}\pi_L^*)_x$	2762	-	19	41	10	2569	$1.1 \cdot 10^8$
$^1(\pi_H\pi_L^*) \rightsquigarrow ^3(\pi_{H-1}\pi_L^*)_x$	2762	-	19	41	100	26325	$9.5 \cdot 10^7$
$^1(\pi_H\pi_L^*) \rightsquigarrow ^3(\pi_{H-1}\pi_L^*)_y$	2762	-	19	41	0.1	17	$3.4 \cdot 10^5$
$^1(\pi_H\pi_L^*) \rightsquigarrow ^3(\pi_{H-1}\pi_L^*)_y$	2762	-	19	41	1	257	$6.4 \cdot 10^6$
$^1(\pi_H\pi_L^*) \rightsquigarrow ^3(\pi_{H-1}\pi_L^*)_y$	2762	-	19	41	10	2569	$3.1 \cdot 10^7$
$^1(\pi_H\pi_L^*) \rightsquigarrow ^3(\pi_{H-1}\pi_L^*)_y$	2762	-	19	41	100	26325	$2.9 \cdot 10^7$
$^1(\pi_H\pi_L^*) \rightsquigarrow ^3(\pi_{H-1}\pi_L^*)_z$	2762	<0.01	-	41	1	3	$6.9 \cdot 10^1$
$^1(\pi_H\pi_L^*) \rightsquigarrow ^3(\pi_{H-1}\pi_L^*)_z$	2762	<0.01	-	41	10	51	$2.6 \cdot 10^1$
$^1(\pi_H\pi_L^*) \rightsquigarrow ^3(\pi_{H-1}\pi_L^*)_z$	2762	<0.01	-	41	100	627	$5.5 \cdot 10^1$

-
- [1] M. S. Grodowski, B. Veyret and K. Weiss, *Photochem. Photobiol.*, 1977, **26**, 341.
- [2] M. Sikorski and D. Prukala and M. Insińska-Rak and I. Khmelinskii and D. R. Worrall and S. L. Williams and J. Hernando and J. L. Bourdelande and J. Koputa and E. Sikorska, *J. Photochem. Photobiol. A*, 2008, **200**, 148.
- [3] M. Sikorski, E. Sikorska, D. R. Worrall and F. Wilkinson, *J. Chem. Soc. Faraday Trans.*, 1998, **94**, 2347.
- [4] E. Sikorska, I. V. Khmelinskii, D. R. Worrall, J. Koput and M. Sikorski, *J. Fluores.*, 2004, **14**, 57.
- [5] M. Sung, T. A. Moore and P.-S. Song, *J. Am. Chem. Soc.*, 1972, **94**, 1730.
- [6] M. Sikorski, E. Sikorska, F. Wilkinson and R. P. Steer, *Can. J Chem.*, 1999, **77**, 472.
- [7] J. Komasa, J. Rychlewski and J. Koziol, *J. Mol. Struct. (Theochem)*, 1988, **170**, 205.
- [8] R. H. Dekker, B. N. Srinivasan, J. R. Huber and K. Weiss, *Photochem. Photobiol.*, 1973, **18**, 457.
- [9] E. Sikorska, I. V. Khmelinskii, W. Prukala, S. L. Williams, M. Patel, D. R. Worrall, J. L. Bourdelande, J. Koput and M. Sikorski, *J. Phys. Chem. A*, 2004, **108**, 1501.
- [10] A. Toniolo and M. Persico, *J. Chem. Phys.*, 2001, **115**, 1817.
- [11] A. Toniolo and M. Persico, *J. Comput. Chem.*, 2001, **22**, 968.
- [12] B. R. Henry and W. Siebrand, *Organic Molecular Photophysics*, John Wiley & Sons, London, 1973, vol. 1, pp. 153.
- [13] J. Tatchen, N. Gilka and C. M. Marian, *Phys. Chem. Chem. Phys.*, 2007, **9**, 5209.
- [14] S. Salzmann, V. Martinez-Junza, B. Zorn, S. E. Braslavsky, M. Mansurova, C. M. Marian and W. Gärtner, *J. Phys. Chem. A*, 2009, **submitted**.